ACS OMEGA

http://pubs.acs.org/journal/acsodf

Article

Quantitative Proteomic Analysis of Serum Reveals MST1 as a Potential Candidate Biomarker in Spontaneously Diabetic Cynomolgus Monkeys

Chaoyang Tian,* Mingyin Qiu, Haizhou Lv, Feng Yue, and Feifan Zhou

Cite This: *ACS Omega* 2022, 7, 46702−46716

Read Online

ACCESS | Metrics & More | Article Recommendations | Supporting Information

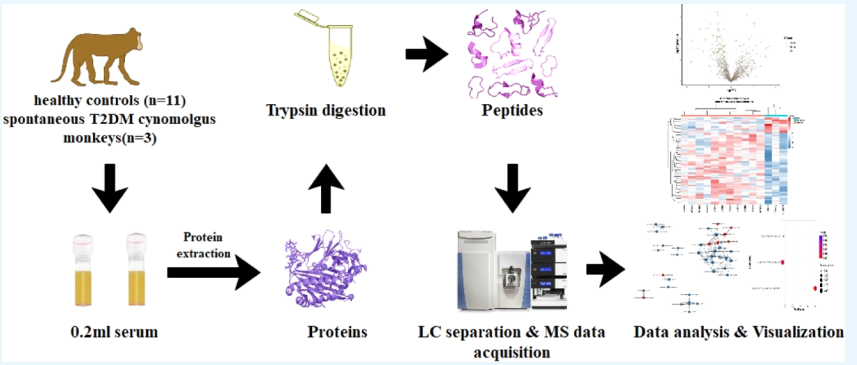

ABSTRACT: The prevalence of type 2 diabetes (T2DM) is increasing globally, creating essential demands for T2DM animal models for the study of disease pathogenesis, prevention, and therapy. A non-human primate model such as cynomolgus monkeys can develop T2DM spontaneously in an age-dependent way similar to humans. In this study, a data-independent acquisition-based quantitative proteomics strategy was employed to investigate the serum proteomic profiles of spontaneously diabetic cynomolgus monkeys compared with healthy controls. The results revealed significant differences in protein abundances. A total of 95 differentially expressed proteins (DEPs) were quantitatively identified in the current study, among which 31 and 64 proteins were significantly upregulated and downregulated, respectively. Bioinformatic analysis revealed that carbohydrate digestion and absorption was the top enriched pathway by the Kyoto Encyclopedia of Genes and Genomes (KEGG) pathway enrichment analysis. Protein−protein interaction network analysis demonstrated that MST1 was identified as the most connected protein in the network and could be considered as the hub protein. MST1 was significantly and inversely associated with FSG and HbA1c. Furthermore, recent lines of evidence also indicate that MST1 acts as a crucial regulator in regulating hepatic gluconeogenesis to maintain metabolic homeostasis while simultaneously suppressing the inflammatory processes. In conclusion, our study provides novel insights into serum proteome changes in spontaneously diabetic cynomolgus monkeys and points out that the dysregulation of several DEPs may play an important role in the pathogenesis of T2DM.

1. INTRODUCTION

Diabetes mellitus (DM) is a metabolic syndrome in which pancreatic β-cells fail to meet the body's need for insulin with resultant hyperglycemia and increased risk of diabetic complications.[1] The IDF (International Diabetes Federation) Diabetes Atlas 10th edition estimates that 536.6 million people globally are living with diabetes (diagnosed or undiagnosed) in 2021, and this number is projected to increase by 46%, reaching 783.2 million by 2045.[2] Type 2 diabetes mellitus (T2DM) also known as adult-onset diabetes or non-insulin-dependent diabetes is the most prevalent type of diabetes, accounting for around 90% of all diabetes cases in the adult population characterized by insulin resistance (IR) and insulin secretion defect.[3] T2DM is associated with abnormalities in energy metabolism arising from increasing age, abdominal obesity, and unhealthy lifestyle.[4] Although the DM has been considered a major global health problem, pathogenesis associated with T2DM is very complex and not completely understood.[5] Thus, research on T2DM management and treatment is now one of the most popular areas of interests. Animal models of diabetes are very useful and beneficial for biomedical studies, as they offer new insights into human diabetes and assist in developing appropriate interventions that

Received: September 2, 2022
Accepted: November 23, 2022
Published: December 6, 2022

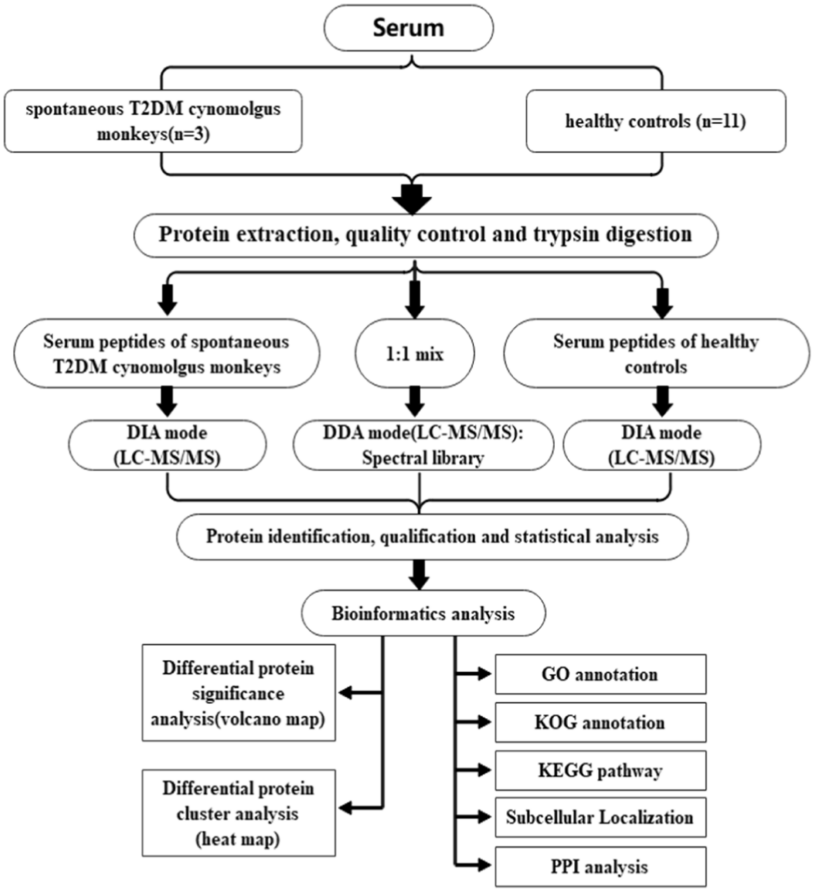

Figure 1. Experimental design and workflow for the comparison of serum proteomic profiles of spontaneously diabetic cynomolgus monkeys and healthy controls using a DIA-based quantitative proteomics technology.

could lead to clinical therapies. To date, rodent models which represent the predominant species in biomedical research have already provided important insights into disease mechanisms, but their predictive value for the efficacy and safety of putative antidiabetic drugs in humans is limited.[6] Similar to humans, non-human primates (NHPs) such as cynomolgus monkeys have an increased propensity to developing DM spontaneously, particularly T2DM relative to increasing age.[7] NHP models show most of the same symptoms as humans, and polygenic models may replicate human diseases. Therefore, NHP models can be treated as a critical translational bridge between basic studies in rodent models and clinical studies in humans.[8]

Proteomics is an emerging tool that includes a thorough study of qualitative and quantitative profiling of the proteins present in different types of clinical specimens, including body fluids (serum, urine, cerebrospinal fluid, etc.), tissues, and cells.[9] It can be systematically characterized by a large scale of dynamic changes in protein expression, which can provide fundamental information for the study of various complicated diseases, which in turn, allowing the capacity to unravel new mechanistic explanations and offering a richer source of potential diagnostic and therapeutic biomarkers associated with complex metabolic disorders including T2DM.[10] Furthermore, a data-independent acquisition (DIA)-based quantitative proteomics technology has received much attention in the recent years as it is a new tandem mass spectrometry method that fragments and analyzes all peptide ions within a selected mass-to-charge ratio range, even those with a low abundance. It also has significant advantages for throughput, quantitative accuracy, and reproducibility, which have been applied in research studies on biomarkers and basic and clinical trials for various diseases.[11−13] The serum is the most complex clinical specimen that can be easily obtained, and most proteins secreted by cells are finally released into the blood circulation.[9] Therefore, serum may contain fundamental information related to the pathophysiological status of all tissues and organs. Therefore, serum proteomic analysis is a valuable approach for identifying protein biomarkers to be applied in the early detection, diagnosis, surveillance, and treatment of various diseases, including T2DM.[14]

The primary objective of the current study was to analyze the serum proteomic profiles of spontaneously diabetic cynomolgus monkeys and healthy controls using DIA-based quantitative proteomics technology and identified protein components by showing different abundances between the two groups. These global serum proteomic profiles will provide fundamental information for further detailed investigations of the molecular pathophysiological mechanisms of T2DM.

2. MATERIALS AND METHODS

The overall workflow in this study is presented in Figure 1.

2.1. Materials and Sampling Procedures. Fourteen serum samples from three spontaneous T2DM cynomolgus monkeys, combined with 11 matched healthy cynomolgus monkeys of similar age, were enrolled in this study. The criteria used for screening of spontaneously diabetic cynomolgus monkeys were guided by the American Diabetes Association (ADA): FSG (fasting serum glucose) ≥126 mg/dL (7.0

https://doi.org/10.1021/acsomega.2c05663
ACS Omega 2022, 7, 46702−46716

mmol/L) and HbAlc (hemoglobin A1c) ≥ 6.5%. The FSG and HbAlc levels of healthy cynomolgus monkeys are <101 mg/dL (5.6 mmol/L) and <5.7%, respectively. Prediabetes is an almost asymptomatic condition defined as an intermediate state between diabetes and health. The clinical characteristic and biochemical data of the 14 cynomolgus monkeys and the monkey housing conditions have been documented in our previous study[15] and are being followed in this study. All experimental procedures and handling, care, and treatment of the monkeys in the current study were approved by the Institutional Animal Care and Use Committee of Hainan Jingang Biotech Co., Ltd. and were performed according to the guidelines of the Association for Assessment and Accreditation of Laboratory Animal Care. All serum samples were collected, followed by immediate freezing, transferring to the laboratory, and being stored at −80 °C before sending to Shenzhen BGI Co., Ltd., for the follow-up DIA-based quantitative proteomics tests and analysis.

2.2. Protein Extraction, Quality Control, and Digestion. Approximately 100 μL of serum sample was transferred into a 5 mL centrifuge tube, and 900 μL (nine times the volume of the serum sample) of SDS-free protein lysate was added into the tube for protein denaturation. The final concentration (10 mM) of DTT (Amresco) was added into the sample and bathed in water at 37 °C for 30 min. After returning to room temperature, the final concentration (55 mM) of IAM (Sigma) was added into the sample and reacted in the dark for 30 min at room temperature. Most of the high-abundant serum proteins were depleted, and low-abundant proteins were enriched using the Cleanert-PEP (polar-enhanced polymer) SPE (solid-phase extraction) column. The extracted and purified protein samples were further re-dissolved using 25 μL of 50 mM NH_4HCO_3, vortexed for 1 min, and then centrifuged for another 1 min. Finally, the protein concentrations were determined with the Bradford assay (Bio-Rad, Hercules, CA, USA),[16] and the purity of the extracted proteins was verified by SDS-PAGE on 12% of gels, followed by Coomassie blue staining.

As for protein digestion, each protein sample (100 μg) was diluted four times using 50 mM NH_4HCO_3 and then digested for 4 h at 37 °C in 2.5 μg of trypsin (trypsin/protein = 1:40(v/v); Promega). Enzymatic peptides were desalted with a Strata X column and vacuum-dried prior to the MS process.

2.3. High pH Reversed-Phase Separation. All samples were equally mixed, and the mixture was diluted in mobile phase A (5% ACN, pH 9.8) and injected onto a Shimadzu LC-20AB HPLC system. A Gemini high pH C18 column (5 μm, 4.6 × 250 mm) was used for liquid-phase separation of samples. Gradient elution was applied with conditions described as follows: flow rate of 1 mL/min: 5% mobile phase B (95% ACN, pH 9.8) for 10 min, 5−35% mobile phase B for 40 min, 35−95% mobile phase B for 1 min, flow phase B lasted 3 min, and 5% mobile phase B equilibrated for 10 min. The elution peaks were monitored at a wavelength of 214 nm, and the fractions were collected every minute. Finally, the peptide components were combined into a total of 10 fractions, which were then freeze-dried.

2.4. Data-Dependent Acquisition and Data-Independent Acquisition Analysis. The dried peptide sample was re-dissolved with mobile phase A (2% ACN and 0.1% FA) and centrifuged at 20,000*g* for 10 min, and the supernatant was taken for injection. Separation was performed on a Thermo UltiMate 3000 UHPLC liquid chromatograph. The sample was first enriched in the trap column and desalted, followed by entering into a tandem self-packed C18 column (150 μm internal diameter, 1.8 μm column size, and 35 cm column length). Peptides were separated at a flow rate of 500 nL/min by the following effective gradients: 0−5 min, 5% mobile phase B (98% ACN and 0.1% FA); 5−120 min, 5−25% mobile phase B; 120−160 min, 25−35% mobile phase B; 160−170 min, 35−80% mobile phase B; 170−175 min, 80% mobile phase B; and 175−180 min, 5% mobile phase B. The nanoliter liquid phase separation end was directly connected to the mass spectrometer, and the peptides separated by the liquid phase were sprayed into the nanoESI source and then allowed to enter a Q-Exactive HF X (Thermo Fisher Scientific, San Jose, CA) tandem mass spectrometer for data-dependent acquisition (DDA) and data-independent acquisition (DIA) analyses.

The DDA MS parameters were set as follows: ion source voltage 1.9 kV, MS scanning range m/z 350−1500; MS resolution 120,000, maximal injection time (MIT) 100 ms; MS/MS collision type HCD, collision energy NCE 28; MS/MS resolution 30,000; MIT 100 ms; and dynamic exclusion duration 30 s. The start m/z for MS/MS was fixed to 100. The precursor for MS/MS scan was satisfied: charge range from 2+ to 6+ and top 20 precursors with intensity over 5×10^4. AGC was set as follows: MS 3×10^6 and MS/MS 1×10^5.

The DIA MS parameters were set as follows: ion source voltage 1.9 kV, MS scanning range m/z 400−1250; MS resolution 120,000; and MIT 50 ms. For MS/MS scan, the scanning range m/z 400−1250 was equally divided into 45 continuous windows, and fragment ions were scanned in an Orbitrap with a resolution of 30,000. The MS/MS collision type was also selected as HCD, and MIT was in the auto mode. The collision energy was in the distributed mode: 22.5, 25, and 27.5, AGC was set as 1×10^6.

2.5. Protein Identification and Quantitative Analysis. DDA data were processed and analyzed by MaxQuant (version 1.5.3.30). The peptide/protein entries that satisfied FDR (false discovery rate) ≤ 1% were used to construct the final spectral library, and the retrieved database was Uniprot_mcf_irt.fasta (77,481 sequences). Parameters are listed as follows: (1) enzyme: trypsin; (2) minimal peptide length: 7; (3) FDR at the protein and PSM level: 0.01; (4) fixed modifications: carbamidomethyl (C); (5) variable modifications: oxidation (M); acetyl (protein N-term); glutamine (Q) to pyro-glutamate (N-term Q); and deamidated (NQ). The DIA MS data were analyzed by the Spectronaut (version 12.0.20491.14.21367), which uses iRT peptides for retention time (RT) calibration. Based on the Target-decoy model applicable to sequential window acquisition of all theoretical mass spectra (SWATH-MS), the false-positive control was performed with 1% of FDR. Finally, the significant differences of serum proteome were statistically analyzed by MSstats (version 3.2.1).[17] After carrying out error correction and normalization on each sample, the DEPs between the groups were selected according to the absolute value of fold change (|FC|) ≥ 1.5 and p value < 0.05 as the criteria for significant differences. The mass spectrometry proteomics data have been deposited to the ProteomeXchange Consortium via the PRIDE[18] partner repository with the dataset identifier PXD036971.

2.6. Bioinformatics Analysis. Identified DEPs were annotated and classified into the pathway by Gene Ontology (GO) (http://www.geneontology.org) and the Kyoto Encyclopedia of Genes and Genomes (KEGG) PATHWAY

https://doi.org/10.1021/acsomega.2c05663
ACS Omega 2022, 7, 46702−46716

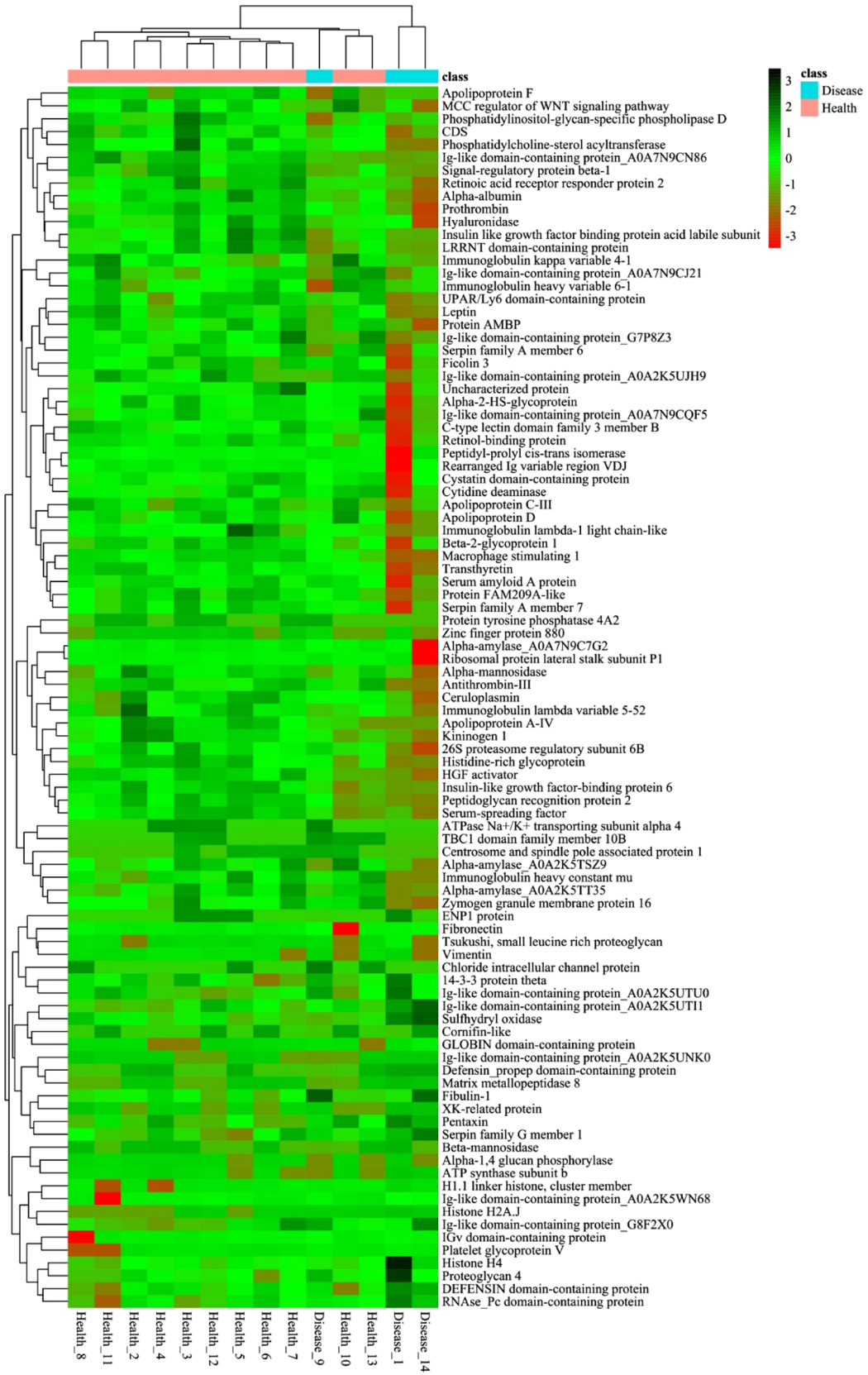

Figure 2. Cluster analysis of the identified DEPs. The *X*-axis of the graph is the sample names, and the *Y*-axis is the protein names which can also be downloaded from https://www.uniprot.org/. Since several protein IDs are matching the same protein names, these protein names are added with the protein IDs in the graph to distinguish from each other. Heatmap showed the clustered data, where each colored cell represents a protein abundance value. Black represents proteins with a higher expression level, red represents proteins with a lower expression level, and green represents proteins with an intermediate expression level.

https://doi.org/10.1021/acsomega.2c05663
ACS Omega 2022, 7, 46702−46716

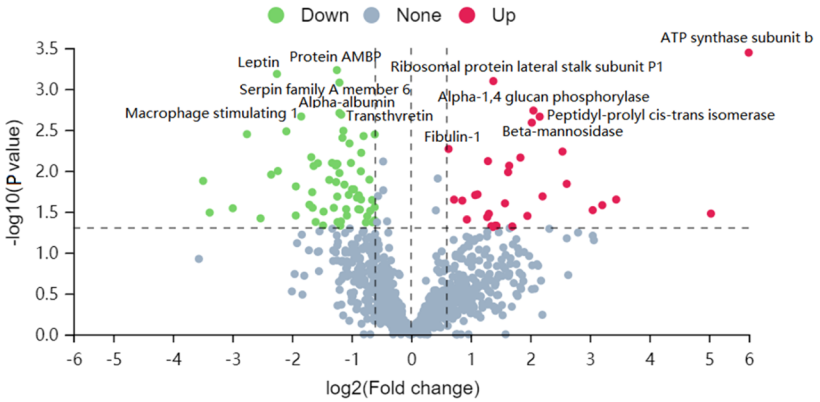

Figure 3. Volcano plot. The *X*-axis of the graph is the protein fold change (T2DM/control) (log2), and the *Y*-axis is the corresponding −log10 (*P*-value). The red dots indicate the significantly upregulated proteins, the green dots indicate the significantly downregulated proteins, and the gray dots indicate proteins without significant changes. The protein names of the top six DEPs based on the *P* value of upregulated (ATP synthase subunit b, ribosomal protein lateral stalk subunit P1, α-1,4 glucan phosphorylase, peptidyl-prolyl cis−trans isomerase, β-mannosidase, and fibulin-1) and downregulated (protein AMBP, leptin, serpin family A member 6, α-albumin, TTR, and macrophage stimulating 1) proteins are marked on the figure, respectively.

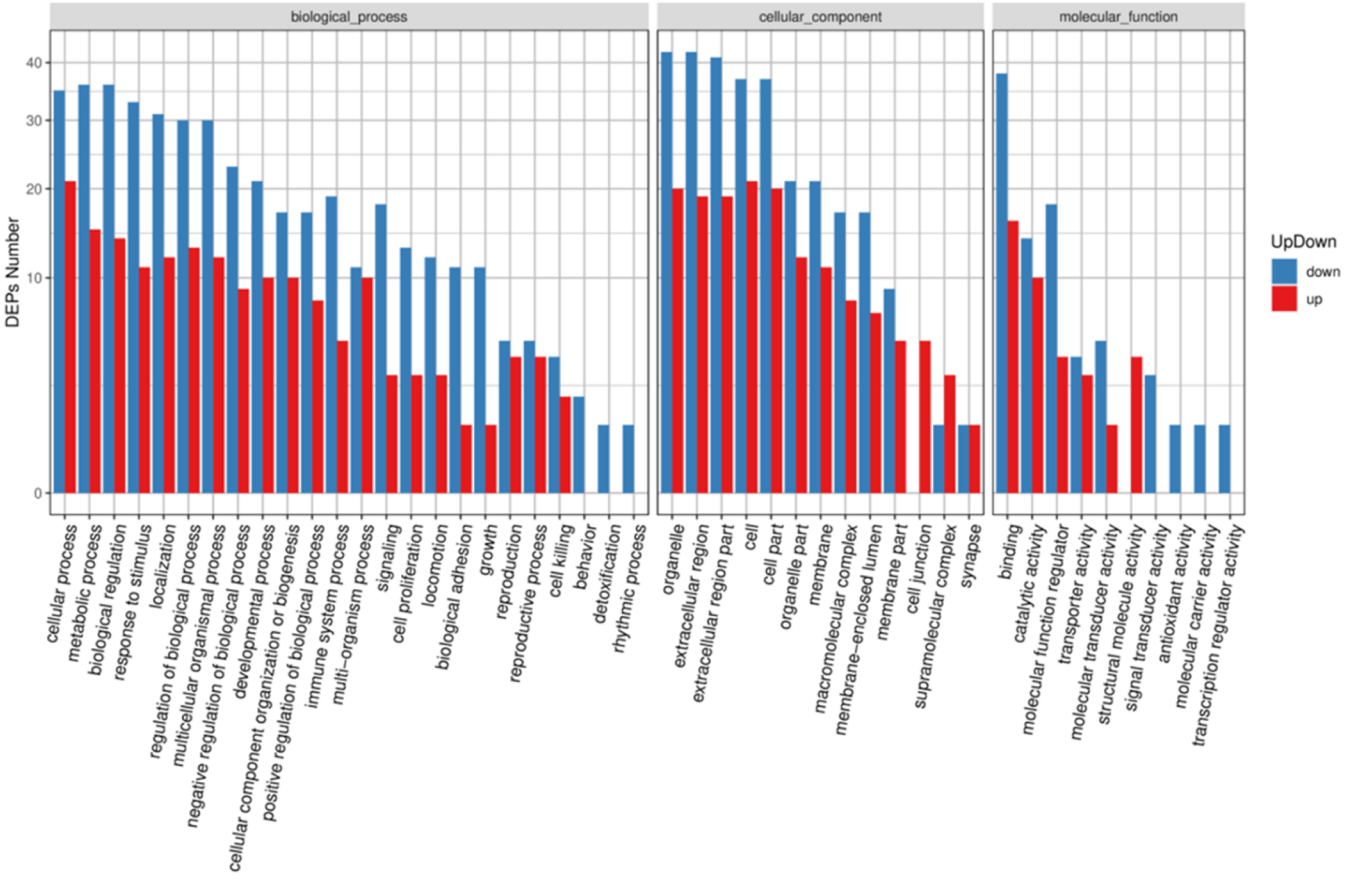

Figure 4. Up- or downregulation of differential proteins in GO punctuational classification. The *X*-axis represents the GO annotation entry and the *Y*-axis represents the number of differential proteins with up- or downregulation.

database (http://www.genome.jp/kegg/pathway.html), respectively. The possible functions of serum proteins were predicted by Eukaryotic Orthologous Groups (KOG) software, and the WoLF PSORT software was used to predict the subcellular localization of the identified DEPs. The STRING database (STRING 11.0) was used to perform the protein−protein interaction (PPI) network, which is important to deepen our understanding of the pathogenesis of various diseases and hasten the appropriate interventions.

2.7. Statistical Analysis. All data were expressed as mean ± SD and analyzed using Student's *t*-test to conduct the differences between the two groups. The enumeration data were expressed as the number of samples and the composition ratio and analyzed using either the Pearson's χ-squared test or Fisher's exact test. Statistical significance was set at $p < 0.05$.

https://doi.org/10.1021/acsomega.2c05663
ACS Omega 2022, 7, 46702−46716

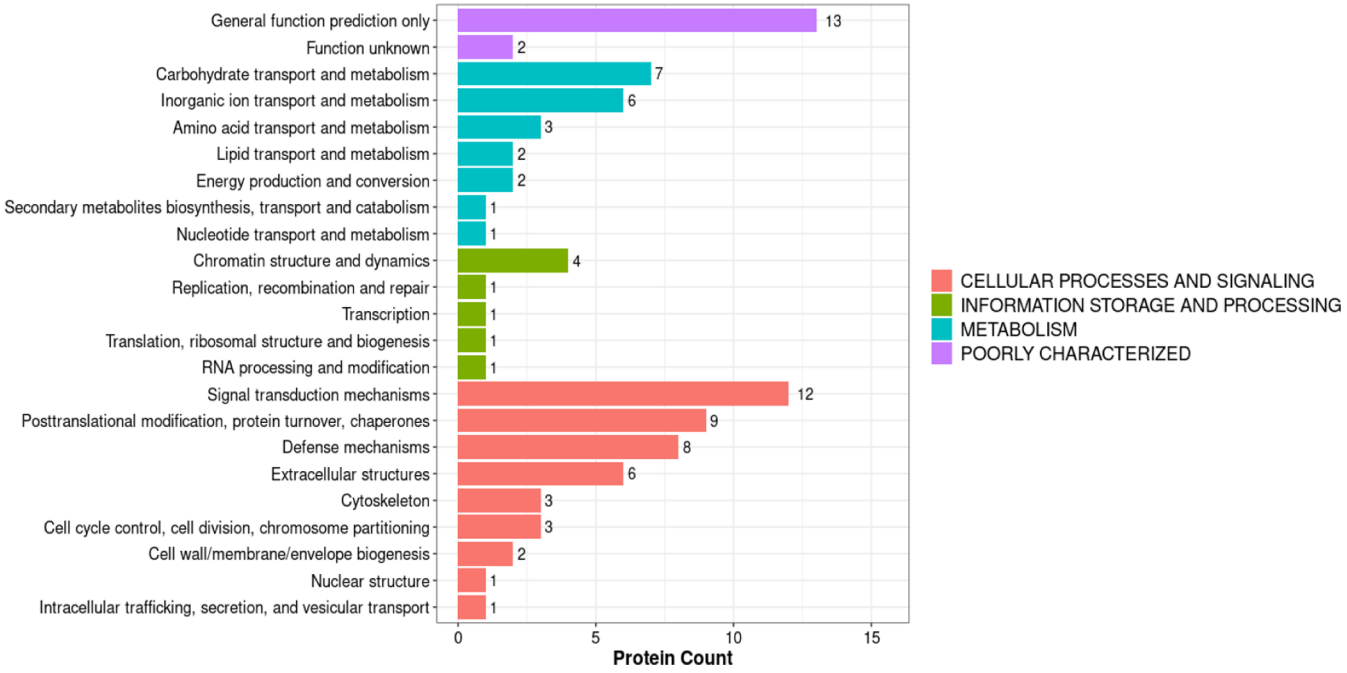

Figure 5. KOG function classification of the DEPs. The *X*-axis displays the DEP count and the *Y*-axis displays the KOG terms.

3. RESULTS

3.1. Characterization of Quantitative Protein Detection. DIA-based proteomic analyses of 14 serum samples of cynomolgus monkeys were carried out in this study. As a result, 8658 peptides and 1021 proteins were tentatively identified (Tables S1 and S2). After calculating the fold change and *P* value through the MSstats software package, 972 proteins were further identified. Two filtration criteria (fold change > 1.50 or fold change < 0.67 and *P* value < 0.05) were used to get significantly differentially expressed proteins (DEPs). Compared with the healthy cynomolgus monkey group (healthy group), a total of 95 DEPs (including 9 DEPs with only one intensity in the disease group) were detected in the spontaneously diabetic cynomolgus monkey group (disease group), of which 31 were upregulated and 64 were downregulated (Figures 2 and 3 and Table S3). Among the upregulated proteins, the ATP synthase subunit b with a *P*-value of 3.6×10^{-4} showed the greatest difference between the two groups. The ATP synthase subunit b belongs to the mitochondrial ATPase complex catalytic core to produce ATP and plays an important role in maintaining the energy homeostasis in the cells. Among the downregulated proteins, protein AMBP (α-1-microglobulin/bikunin precursor) was the most different protein with a *P*-value of 5.9×10^{-4}. Protein AMBP is the precursor of α-1-microglobulin (A1M) and bikunin, a protein involved in the scavenging and metabolism of free radical and oxidizing residues.

3.2. GO Functional Annotation of the DEPs. GO is an international standard gene function classification system that provides a timely updated standard vocabulary (controlled vocabulary) to comprehensively describe the properties of genes and gene products in organisms. Therefore, GO analysis is widely used to describe the molecular function of protein sets. In the present study, we carried out GO functional annotation analysis of the identified DEPs. Based on these results, we generated GO functional classification maps to discriminate the up- and downregulated proteins (Figure 4 and Table S4). All identified DEPs were analyzed for GO annotation based on the three categories of biological process (BP), cellular component (CC), and molecular function (MF). For GO enrichment analysis for DEPs, 24, 13, and 10 terms were participated in BP, CC, and MF, respectively. In BP, DEPs were mainly involved in the cellular process, metabolic process, and biological regulation. A total of 56 DEPs participated in the cellular process and included 21 upregulated and 35 downregulated proteins. In the cellular process, the most different protein was ATP synthase subunit b with a *P*-value of 3.6×10^{-4}. In CC, DEPs were mainly related to organelle, extracellular region, and extracellular region part categories. A total of 62 DEPs were involved in organelle, with 20 upregulated and 42 downregulated proteins. ATP synthase subunit b with a *P*-value of 3.6×10^{-4} was also the most different protein in the organelle. In MF, DEPs mainly played a role in binding, followed by the catalytic activity and molecular function regulation. A total of 54 DEPs were involved in binding, among which 16 were upregulated and 38 were downregulated. The most different protein was protein AMBP with a *P*-value of 5.9×10^{-4} in binding. In general, the DEPs from the serum samples of spontaneous T2DM cynomolgus monkeys were participated in GO enrichment analysis more extensively.

3.3. KOG Function Classification of the DEPs. We predicted the possible functions of the identified DEPs and generated functional classification statistics by using the Eukaryotic Orthologous Groups (KOG) database, a database for the orthologous classification of eukaryotic proteins. In our KOG functional classification, all the DEPs were annotated into 23 KOG terms (Figure 5 and Table S5). The top-ranked functional clusters included four terms in cellular processes and signaling group (signal transduction mechanisms, posttranslational modification, protein turnover, and chaperones, defense mechanisms, and extracellular structures), followed by two terms in the metabolism group (carbohydrate transport and metabolism and inorganic ion transport and metabolism).

https://doi.org/10.1021/acsomega.2c05663
ACS Omega 2022, 7, 46702−46716

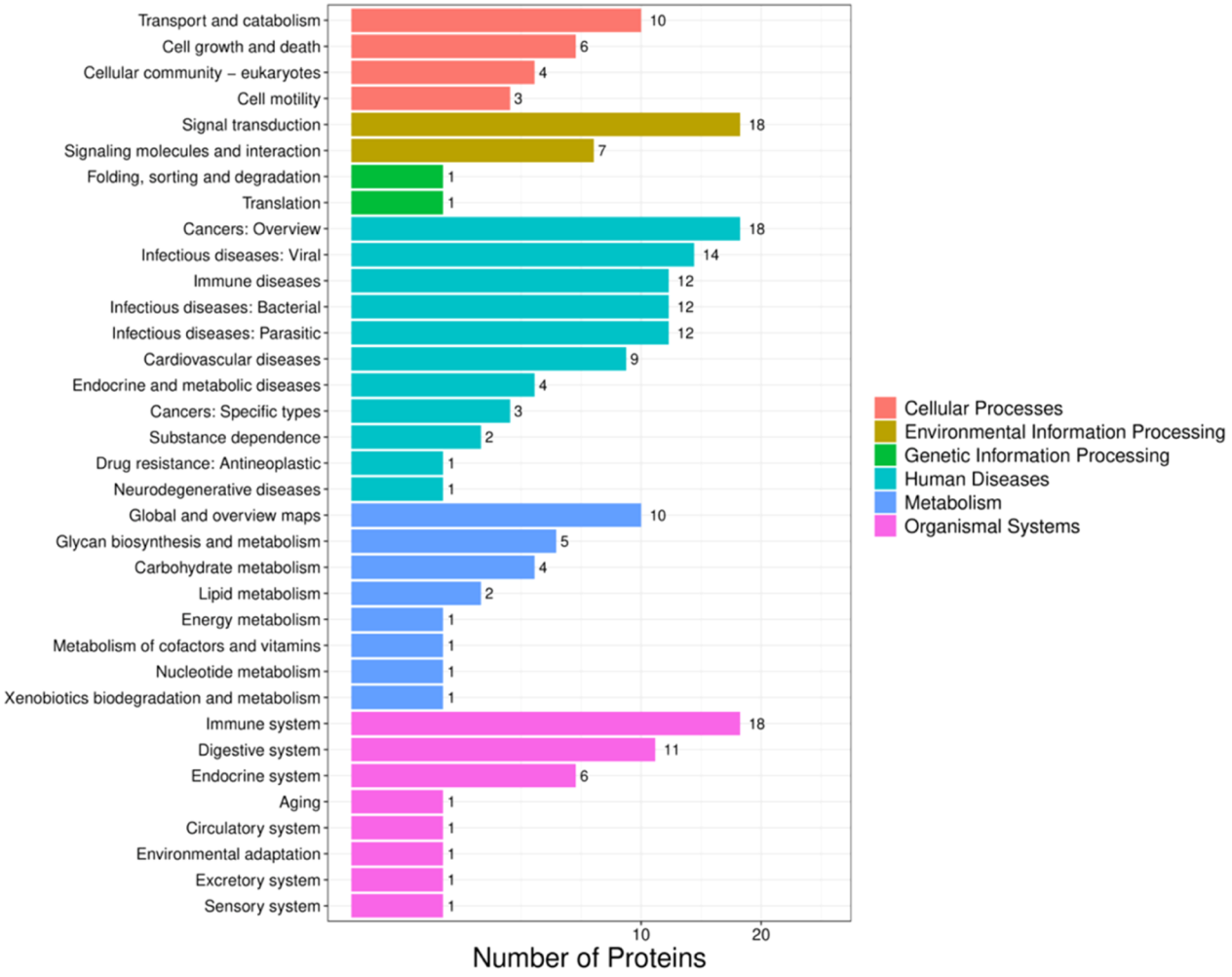

Figure 6. KEGG pathway classification of the DEPs. The *X*-axis displays the DEP count, and the *Y*-axis displays the name of biological functions which were classified into six KEGG pathway categories, including cellular processes, environmental information processing, genetic information processing, human diseases, metabolism, and organismal systems.

3.4. KEGG Pathway Analysis of the DEPs. To explore the functions of the DEPs in physiological or pathological status, we conducted KEGG pathway analysis to further characterize the biological functions of the identified DEPs. As shown in Figure 6 and Table S6, the 95 identified DEPs were involved in 35 pathways, among which the top 8 involving more than 10 proteins were related to signal transduction, cancers, immune system, viral infectious diseases, immune diseases, bacterial infectious diseases, parasitic infectious diseases, and digestive system. All the identified DEPs could also be further divided into six KEGG pathway classification, including cellular processes, environmental information processing, genetic information processing, human diseases, metabolism, and organismal systems. According to the results shown in Figure 7, the upregulated proteins were annotated to 13 major pathways. In turn, downregulated proteins were annotated to 25 major pathways; the more proteins involved pathways were the "PI3K-Akt signaling pathway" and "Epstein−Barr virus infection". Among them, thyroid hormone synthesis, starch and sucrose metabolism, and carbohydrate digestion and absorption were the top three biological functions for the DEP sets (Figure 8), and the most enriched KEGG pathway was carbohydrate digestion and absorption.

3.5. Subcellular Localization of the DEPs. We performed WoLF PSORT software to predict the subcellular localization of the identified DEPs (Figure 9 and Table S7) in the present study. The results demonstrated that the extracellular, nucleus, cytosol, and mitochondria were the most represented structures.

3.6. Protein−Protein Interaction Network of the DEPs. The PPI network analysis can provide valuable information about the interaction between proteins and help to identify core proteins. The interaction relationship of DEPs was evaluated with the STRING PPI database, and the top 100 interactions with confidence was used to construct the interaction map (Figure 10 and Table S8), in which circled nodes represent proteins (red nodes represent proteins with upregulation and blue nodes represent proteins with downregulation), the size of the circle indicates the density of relationship, and the connections between nodes represent protein interactions.

The PPI network of DEPs includes 39 nodes (8 upregulated proteins and 31 downregulated proteins) and 58 edges (interactions). The hub proteins were selected based on its relations with other proteins, and several highly connected proteins were identified, for example, macrophage stimulating 1(MST1), a liver-derived serum glycoprotein involved in cell

https://doi.org/10.1021/acsomega.2c05663
ACS Omega 2022, 7, 46702−46716

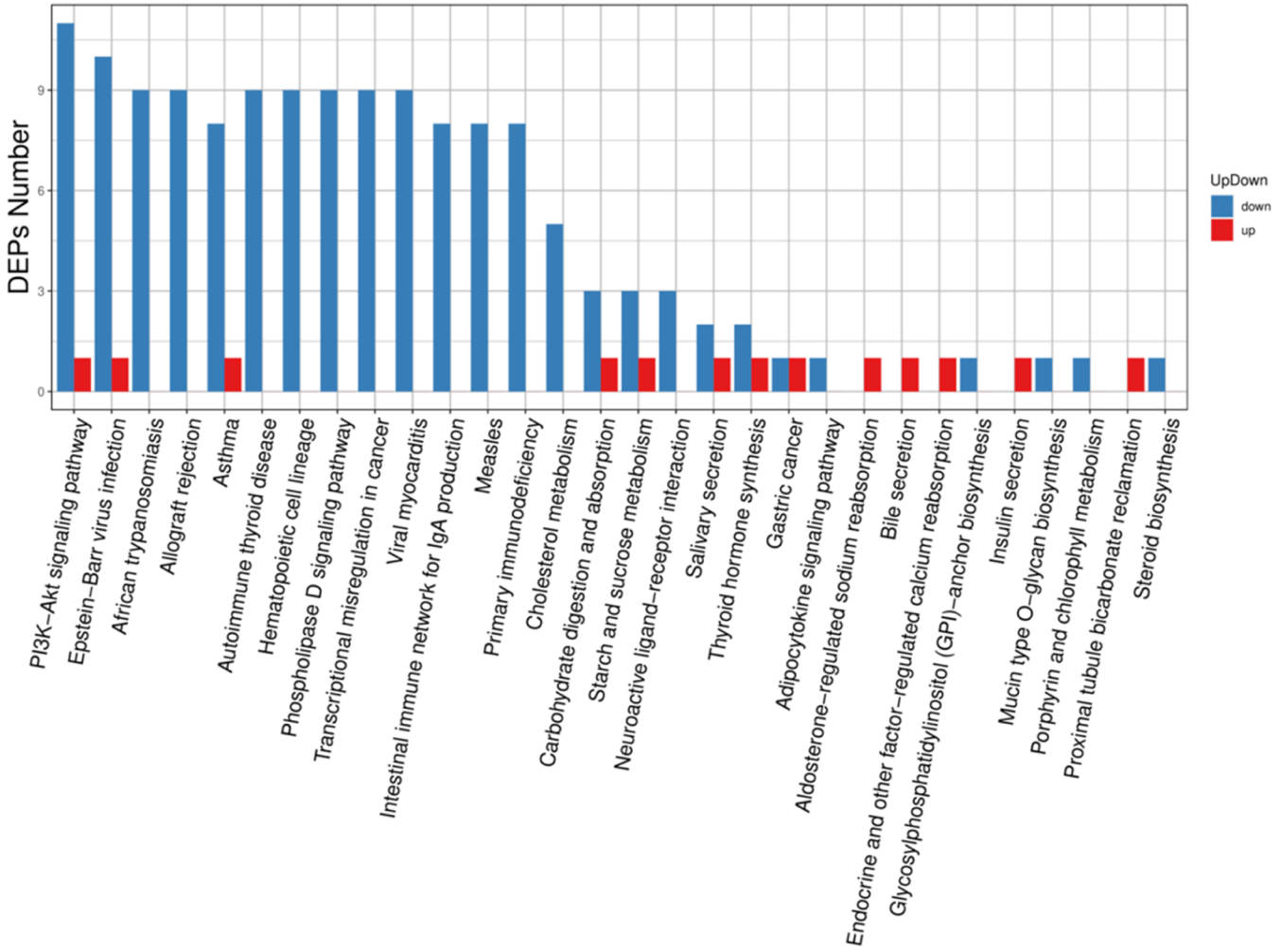

Figure 7. Up- and downregulation differential protein pathway classification. The *X*-axis represents the pathway annotation entry, and the *Y*-axis represents the number of differential proteins with up- or downregulation.

proliferation and differentiation, containing the most edges and representing the top hug protein (highly connected protein with 11 edges). Moreover, apolipoprotein C-III, transthyretin (TTR), α-2-HS-glycoprotein, and serpin family A member 6 were the other hub proteins with eight edges of each.

Furthermore, while analyzing the Pearson correlation coefficient and the significance testing between MST1 and FSG, HbA1c by the Statistical Package for Social Sciences (SPSS 22.0 version), we observed that MST1 was significantly negatively correlated with FSG and HbA1c ($r = -0.782$, $p = 9.42 \times 10^{-4}$ and $r = -0.821$, $p = 3.24 \times 10^{-4}$, respectively) (Figure 11).

4. DISCUSSION

Due to the increase in the prevalence of DM globally, the diabetic animal models are believed to play an important role in elucidating the pathogenesis mechanisms and therapeutic agents of human DM and its complications.[19] Preclinical studies mainly focus on rodent models including rats and especially mice to gain insights into the pathological mechanisms of DM. However, until now, there is no single model which can mimic the development of DM as in humans,[20] and nonrodent models of DM are urgently needed as a valuable supplement to rodents for both practical and physiological reasons with respect to humans.[21] Therefore, numerous lines of evidence highlight the value of NHPs in bridging the translational gap between basic studies in rodents and clinical studies in humans.[22] The NHP model such as the cynomolgus monkey can develop T2DM spontaneously in an age-dependent way which is influenced by overweight and obesity and is characterized by IR, progressive hyperglycemia, and increased inflammation status similar to that observed in human T2DM.[23]

The human T2DM was previously defined using FSG and 2 h serum glucose (PPG) level measured during an oral glucose tolerance test. Although these items have been considered the gold standard for diagnosing diabetes, the disadvantages include the requirement of subject fasting. Glycosylated hemoglobin (HbA1c) is accepted as the best marker of mean glycemia level over the preceding 2−3 months,[24] and the main advantages of the test can be obtained without fasting. Thus, HbA1c with a cut-point ≥6.5% was recommended by the International Expert Committee on the Diagnosis and Classification of Diabetes to diagnose DM in July of 2009 and incorporated into the 2010 American Diabetes Association Standards of Medical Care in Diabetes.[25] Nowadays, the defined diagnostic criteria of cynomolgus monkeys with DM have not been agreed upon.[26−28] Taking the translational medicine into consideration, our study adopted the following T2DM definitions: FSG ≥ 7.0 mmol/L (126 mg/dL) and

https://doi.org/10.1021/acsomega.2c05663
ACS Omega 2022, 7, 46702−46716

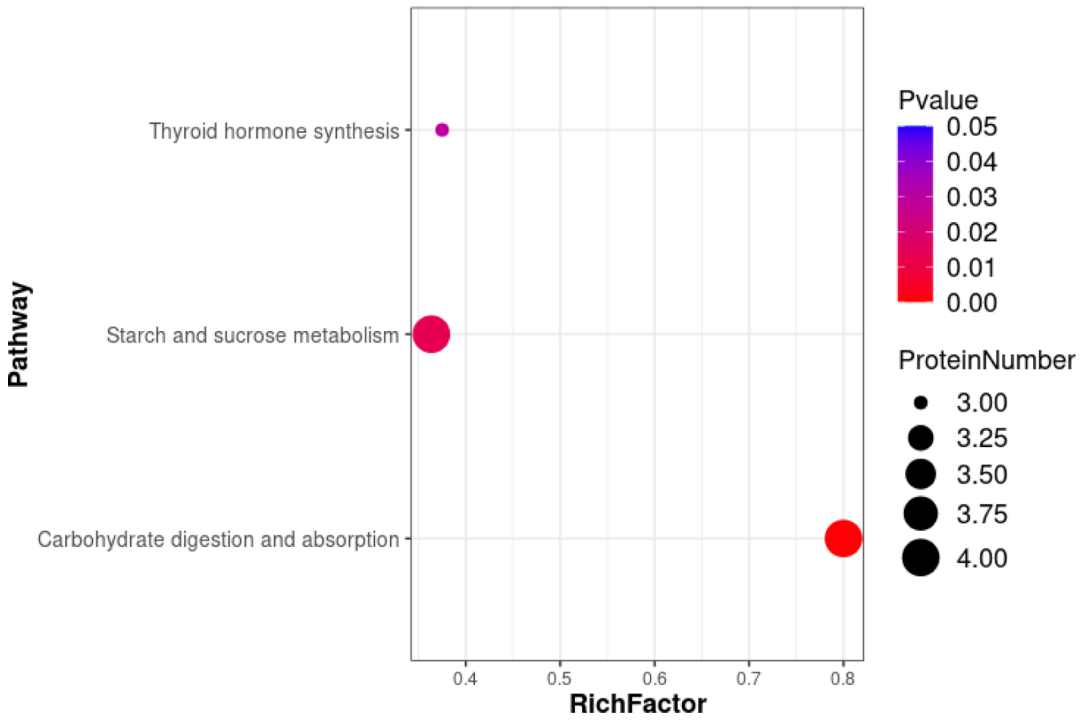

Figure 8. Significantly enriched pathway. This figure shows the metabolic pathway in which the differential proteins are significantly enriched. The *X*-axis shows the enrichment factor (RichFactor) which represents the number of differential proteins annotated to the pathway divided by all the proteins identified in the pathway. The larger the value, indicating the greater the proportion of differential proteins annotated to the pathway. The size of the circle represents the number of differential proteins annotated to the pathway.

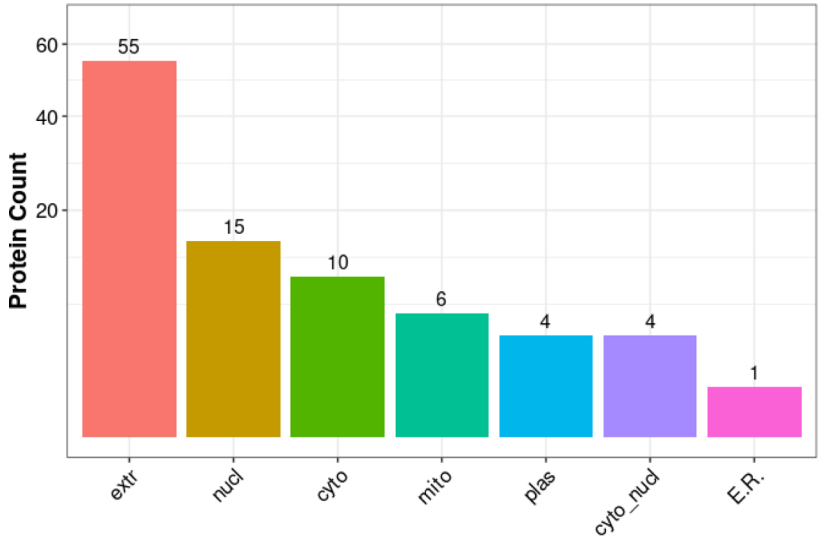

Figure 9. Subcellular localization of the DEPs. The *X*-axis represents the subcellular structure term, and the *Y*-axis represents the protein count.

HbA1c ≥ 6.5%. In the present study, we found three spontaneously type 2 diabetic cynomolgus monkeys within the relatively small sample size which lend credence that a small percentage of cynomolgus monkeys may develop T2DM spontaneously.[29]

Proteomic studies would be capable of fostering a better understanding of disease processes, develop new biomarkers for diagnosis and early detection of disease, discover cellular pathways associated with the disease of interest, and accelerate drug development.[30] As far as we know, this was the first DIA-based proteomic analysis of serum samples of spontaneous T2DM cynomolgus monkeys compared with healthy controls. In the current study, it is aimed to investigate the characteristics of serum proteomic profiles between the two groups, and the results evidenced the alterations of serum proteomic profiles in spontaneous T2DM cynomolgus monkeys. As a result, a total of 95 DEPs were quantitatively identified, among which 31 and 64 proteins were significantly upregulated and downregulated, respectively. Furthermore, we compared the results with human studies and showed some similar results that lower the level of TTR in patients with diabetes compared with normal subjects, although the sample size is very limited.[31]

https://doi.org/10.1021/acsomega.2c05663
ACS Omega 2022, 7, 46702−46716

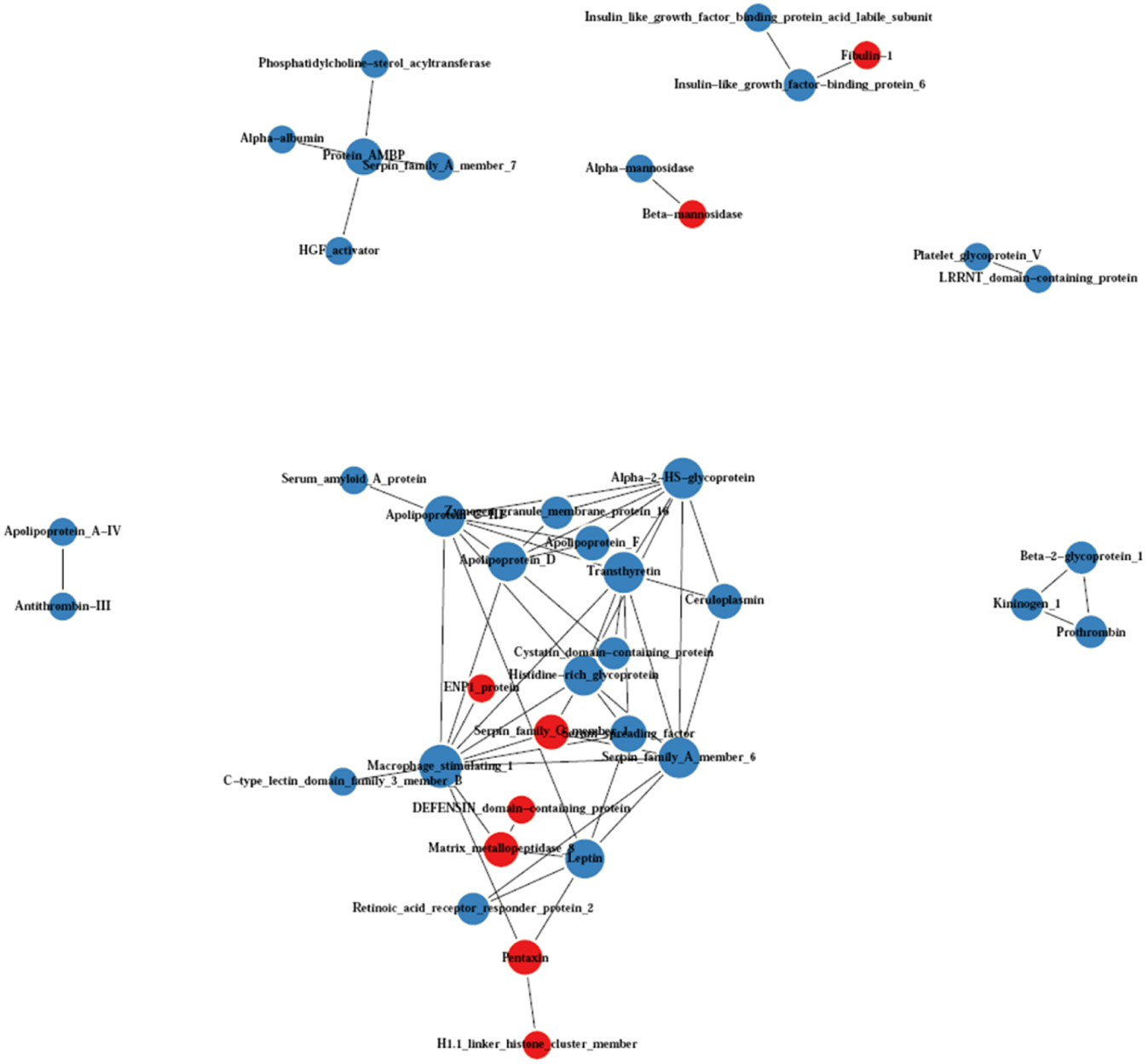

Figure 10. PPI network of the DEPs.

We made an attempt to assign possible functions to the 95 identified DEPs using the GO functional annotation. The functional annotation of gene products, both proteins and RNAs, is a major endeavor that requires a judicious mix of manual analysis and computational tools. GO is one of the most widely used tools for functional annotation, particularly in the analysis of data from high-throughput experiments.[32] In the present study, we showed that the BP of the cellular process, the CC of the organelle, and the MF of the binding gained the highest counts based on GO term analysis. Furthermore, ATP synthase subunit b was the most different protein both in the BP of the cellular process and the CC of the organelle. ATP synthase which is found in the inner membrane of the mitochondria is the central enzyme of energy metabolism in most organisms.[33] In this study, as part of ATP synthase, ATP synthase subunit b was upregulated in the serum of spontaneously diabetic cynomolgus monkeys, implying that the pathogenesis of T2DM might be relevant to the ATP synthesis and energy consumption. In addition, protein AMBP (α-1-microglobulin/bikunin precursor) was the most different protein in the MF of binding. AMBP is a precursor protein processed proteolytically into bikunin and α-1-microglobulin (A1M).[34] A1M is a conserved tissue housekeeping protein secreted from the liver and most other epithelial cells, presented in blood and all tissues at remarkably constant concentrations,[35] and has a physiological role as a protective antioxidant, operating by clearing extravascular fluids of free radicals and heme groups and transporting them to the kidneys for degradation.[36] In this study, protein AMBP was downregulated in the serum of spontaneously diabetic cynomolgus monkeys, implying that the pathogenesis of T2DM might be relevant to oxidative damage, the result that is consistent with the previous research that decreased oxidative capacity and mitochondrial aberrations are major contributors to the development of IR and T2DM.[37]

https://doi.org/10.1021/acsomega.2c05663
ACS Omega 2022, 7, 46702−46716

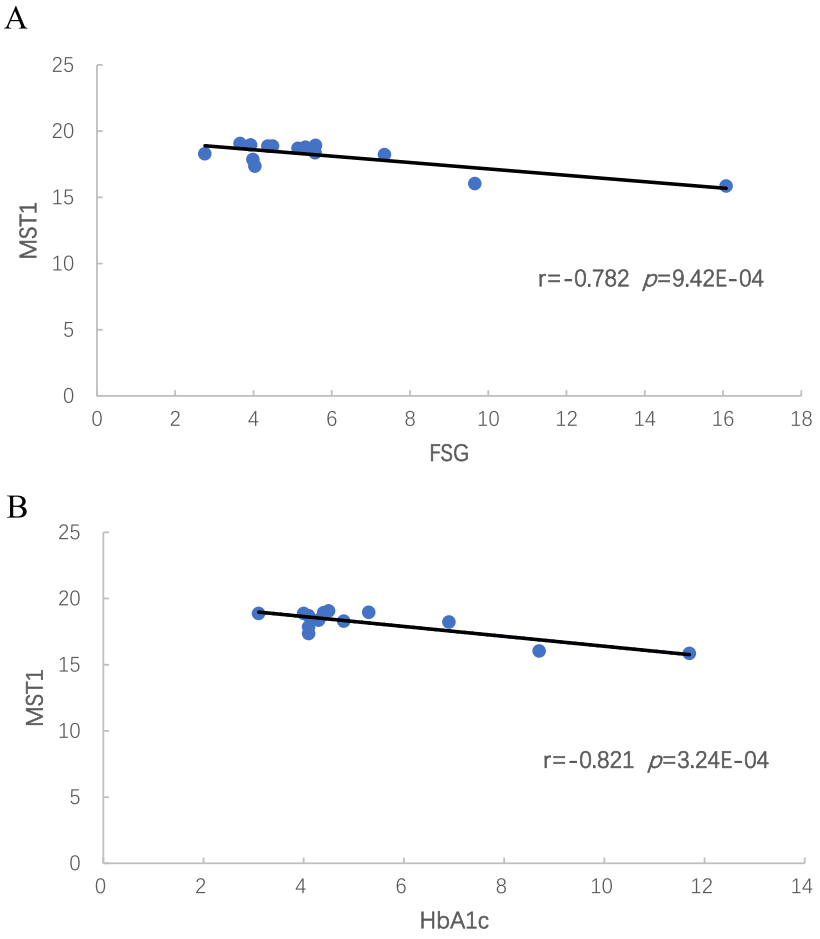

Figure 11. Pearson correlation coefficient (r) and p-value (p) between MST1 and FSG (A) and HbA1c (B) in 14 cynomolgus monkeys, respectively.

Furthermore, we also made an effort to identify the potential signaling pathways that might exist among the DEPs using KEGG pathway analysis, one of the most commonly used method for the integration and interpretation of high-throughput proteomic and genomic data. In the present study, we had discovered three signaling pathways, including carbohydrate digestion and absorption, starch and sucrose metabolism, and thyroid hormone synthesis showing significant enrichment. Among them, the carbohydrate digestion and absorption pathway was the top enriched KEGG pathway. The DEPs involved in this pathway included one upregulated (ATPase Na^+/K^+ transporting subunit α 4) and three downregulated proteins. Interestingly, all these three downregulated proteins were α-amylase, despite the various sequences of amino acids present in them. Na^+/K^+-ATPase, a well-characterized membrane ion transporter composed of two functional subunits (α and β) and one regulatory γ subunit,[38] plays a central role in the regulation of intracellular and extracellular cations (i.e., low Na^+ and high K^+) and cellular homeostasis. Impaired erythrocyte Na^+/K^+-ATPase activity has been implicated in the pathogenesis of DM.[39] The relation of elevated ATPase Na^+/K^+ transporting subunit α 4 and decreased erythrocyte Na^+/K^+-ATPase activity needs to be further elucidated in future studies. α-Amylase is a hydrolase enzyme that catalyzes the hydrolysis of internal α-1,4-glycosidic linkages in starch to yield low molecular weight products such as glucose and maltose, causing postprandial hyperglycemia and blood glucose levels to rise.[40,41] It is regarded as a well-known therapeutic target for antidiabetic agents to design the drug and provide an alternate approach for the treatment of T2DM. Inhibition of this enzyme leads to inhibition of starch breaking and results in lower levels of blood glucose.[42] Whether the downregulated α-amylase in the study was associated with the overnight fasting status needs to be further studied. Additionally, it is of note that the PI3K-Akt signaling pathway was involved with top numbers of DEPs (11 downregulated and 1 upregulated), even though no significant difference was observed between the groups (p = 0.26). Accumulating evidence has shown that the PI3K-Akt signaling pathway plays a critical role in IR, and IR occurs in hepatic cells when the insulin receptor substrate-1 (IRS-1)/phosphatidylinositol 3-kinase (PI3K)/protein kinase B (Akt) signaling pathway is downregulated.[43,44] Thus, the impaired PI3K-Akt signaling pathway caused IR and IR also exacerbated the PI3K-Akt signaling pathway. Finally, the vicious circle would lead to the development of T2DM.[45]

It is well known that proteins usually do not work alone but rather interact with each other to perform various functions. PPI network analysis approaches are a useful strategy for accelerating our understanding of molecular crosstalk and the BPs underlying T2DM pathogenesis, especially due to the complex nature of this disease. For the PPI network, hub proteins are defined as the most connected nodes within the network; thus, they are responsible to sustain network connectivity.[46] It is important to note that macrophage

https://doi.org/10.1021/acsomega.2c05663
ACS Omega 2022, 7, 46702−46716

stimulating 1 (MST1) was the most important hub protein with 11 edges in the PPI network in this study.

MST1, also known as macrophage-stimulating protein (MSP) and hepatocyte growth factor-like protein (HGFL), was originally discovered by Dr. E. J. Leonard in 1976 as an endogenous serum protein that is mainly secreted by the hepatic cells and is released into the circulating blood as a biologically inactive pro-MSP, which is then cleaved by various enzymatic systems to form biologically active proteins occurring during blood coagulation and local inflammation.[47] Thus, MST1 has a chance to meet various cells via the circulating blood and exhibits multiple biological functions, including promoting migration and phagocytosis by activating macrophages and regulating the inflammatory response of macrophages.[48,49] MST1 exerts its biological activities upon binding to its receptor, the transmembrane tyrosine kinase Recepteur d'Origine Nantais (RON; also known as MST1R) which is ubiquitously expressed in different cell types, and is currently the only known receptor for MST1.[50] The MSP-RON signaling pathway exerts multiple biological effects, including generating oncogenic variants and activating downstream pathways, resulting in tumorigenesis, proliferation, angiogenesis, invasion, and resistance to chemotherapy in various types of cancers,[51] exhibiting the anti-inflammatory and anti-lipogenic properties by activating the AMPK signaling pathway in hepatocytes and macrophages,[52] and suppressing hepatic gluconeogenesis which is tightly balanced by opposing stimulatory (glucagon) and inhibitory (insulin) signaling pathways.[53] Our present study demonstrated that MST1 was downregulated in the serum samples of spontaneous T2DM cynomolgus monkeys compared to the healthy controls and significantly high negatively correlated with FSG and HbA1c, respectively. The results of the present study are consistent with one human cohort study (the Cohort on Diabetes and Atherosclerosis Maastricht (CODAM) study), demonstrating that the serum MST1 level tested by ELISA was inversely associated with the FSG concentration.[54] Taken together, in view of the combined involvements in both suppression of inflammation and amelioration of lipid−glucose metabolism, as a potential candidate biomarker, MST1 has a significant research value and can provide novel diagnostic and therapeutic target in the area of metabolic syndrome, including T2DM. Furthermore, spontaneously diabetic cynomolgus monkeys may be the suitable animal models to further evaluate the precise role and the relevant mechanisms of MST1.

Additionally, apolipoprotein C-III, TTR, α-2-HS-glycoprotein, and serpin family A member 6 were the other hub proteins with downregulation in the present study. Apolipoprotein C-III (apoC-III) is a small atherogenic and proinflammatory protein that is synthesized predominantly in the liver and secreted into the plasma and found on the surface of lipoproteins (very low-density lipoprotein, low-density lipoprotein and high-density lipoprotein).[55] As a key regulator of plasma triglyceride levels, apoC-III may also influence the risk of DM, not only by causing hypertriglyceridemia but also by stimulating the apoptosis of pancreatic β-cell, inducing IR, and promoting inflammation.[56] Human studies demonstrated that elevated apoC-III levels were strongly associated with T2DM.[57] Our results were inconsistent with this conclusion, and the explanation may be related to the normal plasma triglyceride levels in both spontaneously diabetic cynomolgus monkeys and the healthy controls. TTR is a highly conserved homotetrameric thyroxine transport protein synthesized predominantly in the liver and choroid plexus and exists in the plasma and/or cerebrospinal fluid of vertebrates and involved in the regulation of glomerular filtration of retinol-binding protein 4 (RBP4) and in the maintenance of the protein level in plasma.[58,59] Many human studies have shown the association between plasma TTR levels and the risk of T2DM, but the results were not consistent with each other; only a few lines of evidence reported that the plasma level of TTR is high in T2DM, but the relation with the diabetic condition is not clear.[60,61] α-2-HS-glycoprotein, also known as fetuin-A (Fet-A), is a hepatic secretory glycoprotein and reversibly binds the insulin receptor tyrosine kinase in the peripheral tissues, thereby inhibiting the insulin-induced intracellular signal cascade and producing peripheral IR.[62] Human prospective studies on Fet-A and incidence of DM have so far yielded contradicting results; some systematic reviews reported an increased risk of T2DM with higher Fet-A concentrations, some other studies opposed the causality of these associations. Serpin family A member 6 is one member of serpin family (serine protease inhibitor), and serpins play significant roles in numerous physiological processes and are known to control key steps in the inflammatory, coagulation, and complement systems.[63] In sum, the possible reasons behind the contradicting results involved in the human and cynomolgus monkey studies could be possibly explained by the differences in species and sample size and variations in detection techniques and analytical methods. Further studies are required to resolve the contradicting findings and explore the underlying mechanisms. Additionally, considering all the above information, the DEPs discussed in the study demonstrated an important role in the pathogenesis of T2DM and provided possible directions for future research studies, including as potential molecular targets for the treatment of DM.

Nonetheless, a few noteworthy limitations of our study should be recognized. First, due to the relative rarity of naturally occurring DM in cynomolgus monkey colonies, the sample size of the study was relatively small. Second, the differential proteins identified were not confirmed with the alternative assays. Therefore, in the future, studies with larger sample sizes should be conducted with permitted conditions, and the targeted proteins are needed to be further verified by other analytical methods such as ELISA assay or multiple reaction monitoring, while the latter is increasingly gaining an advantage over the former method because of its multiplexing capability.[64,65] Last, longitudinal studies may be followed up in pre-diabetic cynomolgus monkeys to identify the predictive value of MST1 on progression to T2DM.

■ ASSOCIATED CONTENT

Supporting Information

The Supporting Information is available free of charge at https://pubs.acs.org/doi/10.1021/acsomega.2c05663.

Summary of peptide identification of spontaneously diabetic cynomolgus monkeys and healthy controls; summary of protein identification of spontaneously diabetic cynomolgus monkeys and healthy controls; whole proteome analyses of spontaneously diabetic cynomolgus monkeys and healthy controls; up- or downregulation of differential proteins in GO function classification; functional KOG classification analysis of

https://doi.org/10.1021/acsomega.2c05663
ACS Omega 2022, 7, 46702−46716

serum DEPs; KEGG enrichment analysis of the identified serum DEPs; subcellular localization of DEPs; and PPI network analysis of DEPs (ZIP)

AUTHOR INFORMATION

Corresponding Author

Chaoyang Tian − *Key Laboratory of Biomedical Engineering of Hainan Province, School of Biomedical Engineering, Hainan University, Haikou, Hainan 570228, China; One Health Institute, Hainan University, Haikou, Hainan 570228, China;* orcid.org/0000-0002-7985-1793; Email: chaoyangtian@hainanu.edu.cn

Authors

Mingyin Qiu − *Animal Experiment Department, Hainan Jingang Biotech Co., Ltd., Haikou, Hainan 571100, China*

Haizhou Lv − *Animal Experiment Department, Hainan Jingang Biotech Co., Ltd., Haikou, Hainan 571100, China*

Feng Yue − *Key Laboratory of Biomedical Engineering of Hainan Province, School of Biomedical Engineering, Hainan University, Haikou, Hainan 570228, China; One Health Institute, Hainan University, Haikou, Hainan 570228, China*

Feifan Zhou − *Key Laboratory of Biomedical Engineering of Hainan Province, School of Biomedical Engineering, Hainan University, Haikou, Hainan 570228, China; One Health Institute, Hainan University, Haikou, Hainan 570228, China*

Complete contact information is available at: https://pubs.acs.org/10.1021/acsomega.2c05663

Notes

The authors declare no competing financial interest.

ACKNOWLEDGMENTS

This work was financially supported by the National Key Research and Development Program of China (2021YFC2600600).

REFERENCES

(1) Hannan, J. M. A.; Ansari, P.; Azam, S.; Flatt, P. R.; Abdel Wahab, Y. H. A. Effects of Spirulina platensis on insulin secretion, dipeptidyl peptidase IV activity and both carbohydrate digestion and absorption indicate potential as an adjunctive therapy for diabetes. *Br. J. Nutr.* **2020**, *124*, 1021−1034.

(2) Sun, H.; Saeedi, P.; Karuranga, S.; Pinkepank, M.; Ogurtsova, K.; Duncan, B. B.; Stein, C.; Basit, A.; Chan, J. C. N.; Mbanya, J. C.; Pavkov, M. E.; Ramachandaran, A.; Wild, S. H.; James, S.; Herman, W. H.; Zhang, P.; Bommer, C.; Kuo, S.; Boyko, E. J.; Magliano, D. J. IDF Diabetes Atlas: Global, regional and country-level diabetes prevalence estimates for 2021 and projections for 2045. *Diabetes Res. Clin. Pract.* **2022**, *183*, 109119.

(3) Egbuna, C.; Awuchi, C. G.; Kushwaha, G.; Rudrapal, M.; Patrick-Iwuanyanwu, K. C.; Singh, O.; Odoh, U. E.; Khan, J.; Jeevanandam, J.; Kumarasamy, S.; Chukwube, V. O.; Narayanan, M.; Palai, S.; Găman, M.-A.; Uche, C. Z.; Ogaji, D. S.; Ezeofor, N. J.; Mtewa, A. G.; Patrick-Iwuanyanwu, C. C.; Kesh, S. S.; Shivamallu, C.; Saravanan, K.; Tijjani, H.; Akram, M.; Ifemeje, J. C.; Olisah, M. C.; Chikwendu, C. J. Bioactive compounds effective against type 2 diabetes mellitus: a systematic review. *Curr. Top. Med. Chem.* **2021**, *21*, 1067−1095.

(4) Hu, C.; Jia, W. Multi-omics profiling: the way towards precision medicine in metabolic diseases. *J. Mol. Cell Biol.* **2021**, *13*, 576−593.

(5) Grubelnik, V.; Zmazek, J.; Markovič, R.; Gosak, M.; Marhl, M. Mitochondrial dysfunction in pancreatic alpha and beta cells associated with type 2 diabetes mellitus. *Life* **2020**, *10*, 348.

(6) Hay, M.; Thomas, D. W.; Craighead, J. L.; Economides, C.; Rosenthal, J. Clinical development success rates for investigational drugs. *Nat. Biotechnol.* **2014**, *32*, 40−51.

(7) Yue, F.; Zhang, G.; Tang, R.; Zhang, Z.; Teng, L.; Zhang, Z. Age- and sex-related changes in fasting plasma glucose and lipoprotein in cynomolgus monkeys. *Lipids Health Dis.* **2016**, *15*, 111.

(8) Zhu, T.; Zeng, W.; Chen, Y.; Zhang, Y.; Sun, J.; Liang, Z.; Yang, Z.; Cheng, W.; Wang, L.; Song, B.; Wu, B.; Wang, F.; Liang, Y.; Gong, L.; Zheng, J.; Gao, F. 2D/3D CMR tissue tracking versus CMR tagging in the assessment of spontaneous T2DM rhesus monkeys with isolated diastolic dysfunction. *BMC Med. Imaging* **2018**, *18*, 47.

(9) Insenser, M.; Escobar-Morreale, H. F. Application of proteomics to the study of polycystic ovary syndrome. *J. Endocrinol. Invest.* **2011**, *34*, 869−875.

(10) Yu, Y.; Tan, P.; Zhuang, Z.; Wang, Z.; Zhu, L.; Qiu, R.; Xu, H. DIA proteomics analysis through serum profiles reveals the significant proteins as candidate biomarkers in women with PCOS. *BMC Med. Genomics* **2021**, *14*, 125.

(11) Zhao, L.; Wu, T.; Li, J.; Cai, C.; Yao, Q.; Zhu, Y. S. Data-independent acquisition-based proteomics analysis correlating type 2 diabetes mellitus with osteoarthritis in total knee arthroplasty patients. *Medicine* **2022**, *101*, No. e28738.

(12) Sun, Y.; Zou, Y.; Jin, J.; Chen, H.; Liu, Z.; Zi, Q.; Xiong, Z.; Wang, Y.; Li, Q.; Peng, J.; Ding, Y. DIA-based quantitative proteomics reveals the protein regulatory networks of floral thermogenesis in Nelumbo nucifera. *Int. J. Mol. Sci.* **2021**, *22*, 8251.

(13) He, A.; Wang, J.; Yang, X.; Liu, J.; Yang, X.; Wang, G.; Li, R. Screening of differentially expressed proteins in placentas from patients with late-onset preeclampsia. *Proteomics: Clin. Appl.* **2022**, *16*, 2100053.

(14) Huang, J.; Yin, X.; Zhang, L.; Yao, M.; Wei, D.; Wu, Y. Serum proteomic profiling in patients with advanced Schistosoma japonicum-induced hepatic fibrosis. *Parasites Vectors* **2021**, *14*, 232.

(15) Tian, C.; Qiu, M.; Lv, H.; Yue, F.; Zhou, F. Preliminary serum and fecal metabolomics study of spontaneously diabetic cynomolgus monkeys based on LC−MS/MS. *J. Med. Primatol.* **2022**, *51*, 355.

(16) Ba, Q.; Hei, Y.; Dighe, A.; Li, W.; Maziarz, J.; Pak, I.; Wang, S.; Wagner, GP; Liu, Y. Proteotype coevolution and quantitative diversity across 11 mammalian species. *Sci. Adv.* **2022**, *8*, No. eabn0756.

(17) Choi, M.; Chang, C. Y.; Clough, T.; Broudy, D.; Killeen, T.; MacLean, B.; Vitek, O. MSstats: an R package for statistical analysis of quantitative mass spectrometry-based proteomic experiments. *Bioinformatics* **2014**, *30*, 2524−2526.

(18) Perez-Riverol, Y.; Bai, J.; Bandla, C.; García-Seisdedos, D.; Hewapathirana, S.; Kamatchinathan, S.; Kundu, D. J.; Prakash, A.; Frericks-Zipper, A.; Eisenacher, M.; Walzer, M.; Wang, S.; Brazma, A.; Vizcaíno, J. A. The PRIDE database resources in 2022: a hub for mass spectrometry-based proteomics evidences. *Nucleic Acids Res.* **2022**, *50*, D543−D552.

(19) Al-Awar, A.; Kupai, K.; Veszelka, M.; Szűcs, G.; Attieh, Z.; Murlasits, Z.; Török, S.; Pósa, A.; Varga, C. Experimental diabetes mellitus in different animal models. *J. Diabetes Res.* **2016**, *2016*, 9051426.

(20) Lai, A. K. W.; Lo, A. C. Animal models of diabetic retinopathy: summary and comparison. *J. Diabetes Res.* **2013**, *2013*, 106594.

(21) Srinivasan, K.; Ramarao, P. Animal models in type 2 diabetes research: an overview. *Indian J. Med. Res.* **2007**, *125*, 451−472.

(22) Abbott, D. H.; Abee, C. R.; Fairbanks, L. A.; Kaplan, J. R.; Marthas, M. L.; Mathieson, B. Demands for rhesus monkeys in biomedical research: a workshop report. *ILAR J.* **2003**, *44*, 222−238.

(23) Chatzigeorgiou, A.; Halapas, A.; Kalafatakis, K.; Kamper, E. The use of animal models in the study of diabetes mellitus. *In Vivo* **2009**, *23*, 245−258.

(24) Koç, Ş.; Baysal, S.; Koç, Z.; Yener, A. Ü. Detection of glycemia and osmolarity changes using eye examinations. *Metab. Syndr. Relat. Disord.* **2018**, *16*, 543−550.

(25) Vable, A. M.; Drum, M. L.; Tang, H.; Chin, M. H.; Lindau, S. T.; Huang, E. S. Implications of the new definition of diabetes for health disparities. *J. Natl. Med. Assoc.* **2011**, *103*, 219−223.

(26) Gu, H.; Liu, Y.; Mei, S.; Wang, B.; Sun, G.; Wang, X.; Xiao, Y.; Staup, M.; Gregoire, FM; Chng, K.; Wang, YJ Left ventricular diastolic dysfunction in nonhuman primate model of dysmetabolism and diabetes. *BMC Cardiovasc. Disord.* **2015**, *15*, 141.
(27) Bezwada, P.; Zhao, J.; Der, K.; Shimizu, B.; Cao, L.; Ahene, A.; Rubin, P.; Johnson, K. A Novel Allosteric Insulin Receptor-Activating Antibody Reduces Hyperglycemia without Hypoglycemia in Diabetic Cynomolgus Monkeys. *J. Pharmacol. Exp. Ther.* **2016**, *356*, 466−473.
(28) Luo, J.; Zhang, H.; Lu, J.; Ma, C.; Chen, T. Antidiabetic effect of an engineered bacterium Lactobacillus plantarum-pMG36e-GLP-1 in monkey model. *Synth. Syst. Biotechnol.* **2021**, *6*, 272−282.
(29) Wu, D.; Yue, F.; Zou, C.; Chan, P.; Alex Zhang, Y. Analysis of glucose metabolism in cynomolgus monkeys during aging. *Biogerontology* **2012**, *13*, 147−155.
(30) Hanash, S. Disease proteomics. *Nature* **2003**, *422*, 226−232.
(31) Chen, Z. Z.; Gerszten, R. E. Metabolomics and proteomics in type 2 diabetes. *Circ. Res.* **2020**, *126*, 1613−1627.
(32) Reference Genome Group of the Gene Ontology Consortium. The Gene Ontology's Reference Genome Project: a unified framework for functional annotation across species. *PLoS Comput. Biol.* **2009**, *5*, No. e1000431.
(33) Weber, J. ATP synthase: Subunit-subunit interactions in the stator stalk. *Biochim. Biophys. Acta, Bioenerg.* **2006**, *1757*, 1162−1170.
(34) Åkerström, B.; Gram, M. A1M, an extravascular tissue cleaning and housekeeping protein. *Free Radicals Biol. Med.* **2014**, *74*, 274−282.
(35) Åkerström, B.; Lögdberg, L. An intriguing member of the lipocalin protein family: α1-microglobulin. *Trends Biochem. Sci.* **1990**, *15*, 240−243.
(36) Olsson, M. G.; Allhorn, M.; Bülow, L.; Hansson, S. R.; Ley, D.; Olsson, M. L.; Schmidtchen, A.; Åkerström, B. Pathological Conditions Involving Extracellular Hemoglobin: Molecular Mechanisms, Clinical Significance, and Novel Therapeutic Opportunities for α1-Microglobulin. *Antioxid. Redox Signaling* **2012**, *17*, 813−846.
(37) Schrauwen, P.; Hesselink, M. K. Oxidative capacity, lipotoxicity, and mitochondrial damage in type 2 diabetes. *Diabetes* **2004**, *53*, 1412−1417.
(38) Kaplan, J. H. Biochemistry of Na,K-ATPase. *Annu. Rev. Biochem.* **2002**, *71*, 511−535.
(39) Konukoglu, D.; Kemerli, G. D.; Sabuncu, T.; Hatemi, H. Relation of erythrocyte Na+-K+ ATPase activity and cholesterol and oxidative stress in patients with type 2 diabetes mellitus. *Clin. Invest. Med.* **2003**, *26*, 279−284.
(40) Souza, P. M. D.; Magalhães, P. D. O. Application of microbial α-amylase in industry - A review. *Braz. J. Microbiol.* **2010**, *41*, 850−861.
(41) Kaur, N.; Kumar, V.; Nayak, S. K.; Wadhwa, P.; Kaur, P.; Sahu, S. K. Alpha-amylase as molecular target for treatment of diabetes mellitus: A comprehensive review. *Chem. Biol. Drug Des.* **2021**, *98*, 539−560.
(42) Bashary, R.; Vyas, M.; Nayak, S. K.; Suttee, A.; Verma, S.; Narang, R.; Khatik, G. L. An insight of alpha-amylase inhibitors as a valuable tool in the management of type 2 diabetes mellitus. *Curr. Diabetes Rev.* **2020**, *16*, 117−136.
(43) Li, Y.; Tang, Y.; Shi, S.; Gao, S.; Wang, Y.; Xiao, D.; Chen, T.; He, Q.; Zhang, J.; Lin, Y. Tetrahedral framework nucleic acids ameliorate insulin resistance in type 2 diabetes mellitus via the PI3K/Akt pathway. *ACS Appl. Mater. Interfaces* **2021**, *13*, 40354−40364.
(44) Wang, J.; He, Y.; Yu, D.; Jin, L.; Gong, X.; Zhang, B. Perilla oil regulates intestinal microbiota and alleviates insulin resistance through the PI3K/AKT signaling pathway in type-2 diabetic KKAy mice. *Food Chem. Toxicol.* **2020**, *135*, 110965.
(45) Huang, X.; Liu, G.; Guo, J.; Su, Z. The PI3K/AKT pathway in obesity and type 2 diabetes. *Int. J. Biol. Sci.* **2018**, *14*, 1483.
(46) Pavlopoulos, G. A.; Secrier, M.; Moschopoulos, C. N.; Soldatos, T. G.; Kossida, S.; Aerts, J. Using graph theory to analyze biological networks. *BioData Min.* **2011**, *4*, 10.
(47) Wang, M. H.; Zhou, Y. Q.; Chen, Y. Q. Macrophage-stimulating protein and RON receptor tyrosine kinase: potential regulators of macrophage inflammatory activities. *Scand. J. Immunol.* **2002**, *56*, 545−553.
(48) Jeong, B. C.; Oh, S. H.; Lee, M. N.; Koh, J. T. Macrophage-Stimulating Protein Enhances Osteoblastic Differentiation via the Recepteur d'Origine Nantais Receptor and Extracellular Signal-Regulated Kinase Signaling Pathway. *J. Bone Metab.* **2020**, *27*, 267−279.
(49) Huang, L.; Fang, X.; Shi, D.; Yao, S.; Wu, W.; Fang, Q.; Yao, H. MSP-RON pathway: potential regulator of inflammation and innate immunity. *Front. Immunol.* **2020**, *11*, 569082.
(50) Li, J.; Chanda, D.; Shiri-Sverdlov, R.; Neumann, D. MSP: an emerging player in metabolic syndrome. *Cytokine Growth Factor Rev.* **2015**, *26*, 75−82.
(51) Yao, H. P.; Zhou, Y. Q.; Zhang, R.; Wang, M. H. MSP-RON signalling in cancer: pathogenesis and therapeutic potential. *Nat. Rev. Cancer* **20132013**, *13*, 466−481.
(52) Chanda, D.; Li, J.; Oligschlaeger, Y.; Jeurissen, M. L.; Houben, T.; Walenbergh, S.; Shiri-Sverdlov, R.; Neumann, D. MSP is a negative regulator of inflammation and lipogenesis in ex vivo models of non-alcoholic steatohepatitis. *Exp. Mol. Med.* **2016**, *48*, No. e258.
(53) Chanda, D.; Li, T.; Song, K. H.; Kim, Y. H.; Sim, J.; Lee, C. H.; Chiang, J. Y. L.; Choi, H.-S. Hepatocyte growth factor family negatively regulates hepatic gluconeogenesis via induction of orphan nuclear receptor small heterodimer partner in primary hepatocytes. *J. Biol. Chem.* **2009**, *284*, 28510−28521.
(54) Li, J. Macrophage stimulating protein (MSP) is inversely associated with fasting plasma glucose: The CODAM Study. *Macrophage Stimulating Protein (MSP) in the Metabolic Syndrome*; Maastricht University, 2017; Vol. *71*. DOI: 10.26481/dis.20170908jl.
(55) Sundaram, M.; Zhong, S.; Khalil, M. B.; Links, P. H.; Zhao, Y.; Iqbal, J.; Hussain, M. M.; Parks, R. J.; Wang, Y.; Yao, Z. Expression of apolipoprotein C-III in McA-RH7777 cells enhances VLDL assembly and secretion under lipid-rich conditions. *J. Lipid Res.* **2010**, *51*, 150−161.
(56) Aroner, S. A.; Yang, M.; Li, J.; Furtado, J. D.; Sacks, F. M.; Tjønneland, A.; Overvad, K.; Cai, T.; Jensen, M. K. Apolipoprotein C-III and high-density lipoprotein subspecies defined by apolipoprotein C-III in relation to diabetes risk. *Am. J. Epidemiol.* **2017**, *186*, 736−744.
(57) Graham, M. J.; Lee, R. G.; Bell, T. A., III; Fu, W.; Mullick, A. E.; Alexander, V. J.; Singleton, W.; Viney, N.; Geary, R.; Su, J.; Baker, B. F.; Burkey, J.; Crooke, S. T.; Crooke, R. M. Antisense oligonucleotide inhibition of apolipoprotein C-III reduces plasma triglycerides in rodents, nonhuman primates, and humans. *Circ. Res.* **2013**, *112*, 1479−1490.
(58) Emdin, M.; Aimo, A.; Rapezzi, C.; Fontana, M.; Perfetto, F.; Seferović, P. M.; Barison, A.; Castiglione, V.; Vergaro, G.; Giannoni, A.; Passino, C.; Merlini, G. Treatment of cardiac transthyretin amyloidosis: an update. *Eur. Heart J.* **2019**, *40*, 3699−3706.
(59) Li, R.-N.; Shen, P.-T.; Lin, H. Y.-H.; Liang, S.-S. Shotgun proteomic analysis using human serum from type 2 diabetes mellitus patients. *Int. J. Diabetes Dev. Countries* **2022**, DOI: 10.1007/s13410-021-01038-z.
(60) Hu, X.; Guo, Q.; Wang, X.; Wang, Q.; Chen, L.; Sun, T.; Li, P.; Shan, Z.; Liu, L.; Gao, C.; Rong, Y. Plasma Transthyretin Levels and Risk of Type 2 Diabetes Mellitus and Impaired Glucose Regulation in a Chinese Population. *Nutrients* **2022**, *14*, 2953.
(61) Pullakhandam, R.; Palika, R.; Ghosh, S.; Reddy, G. B. Contrasting effects of type 2 and type 1 diabetes on plasma RBP4 levels: the significance of transthyretin. *IUBMB Life* **2012**, *64*, 975−982.
(62) Jensen, M. K.; Bartz, T. M.; Djoussé, L.; Kizer, J. R.; Zieman, S. J.; Rimm, E. B.; Siscovick, D. S.; Psaty, B. M.; Ix, J. H.; Mukamal, K. J. Genetically Elevated Fetuin-A Levels, Fasting Glucose Levels, and Risk of Type 2 Diabetes. *Diabetes Care* **2013**, *36*, 3121−3127.
(63) Wang, D.; Gou, M.; Hou, J.; Pang, Y.; Li, Q. The role of serpin protein on the natural immune defense against pathogen infection in Lampetra japonica. *Fish Shellfish Immunol.* **2019**, *92*, 196−208.

https://doi.org/10.1021/acsomega.2c05663
ACS Omega 2022, 7, 46702−46716

(64) Arora, A.; Patil, V.; Kundu, P.; Kondaiah, P.; Hegde, A. S.; Arivazhagan, A. Serum biomarkers identification by iTRAQ and verification by MRM: S100A8/S100A9 levels predict tumor-stroma involvement and prognosis in Glioblastoma. *Sci. Rep.* **2019**, *9*, 2749.
(65) Tuerxunyiming, M.; Xian, F.; Zi, J.; Yimamu, Y.; Abuduwayite, R.; Ren, Y.; Li, Q.; Abudula, A.; Liu, S.; Mohemaiti, P. Quantitative evaluation of serum proteins uncovers a protein signature related to Maturity-Onset Diabetes of the Young (MODY). *J. Proteome Res.* **2018**, *17*, 670−679.

https://doi.org/10.1021/acsomega.2c05663
ACS Omega 2022, 7, 46702−46716